(19)

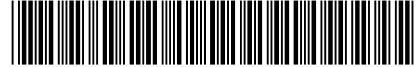

(11) **EP 3 942 262 B1**

(12) **EUROPEAN PATENT SPECIFICATION**

(45) Date of publication and mention of the grant of the patent:
16.08.2023 Bulletin 2023/33

(21) Application number: **19925359.2**

(22) Date of filing: **18.04.2019**

(51) International Patent Classification (IPC):
G01H 9/00 (2006.01) ***H04R 23/00*** (2006.01)
H04R 1/08 (2006.01) ***H04R 7/04*** (2006.01)

(52) Cooperative Patent Classification (CPC):
H04R 23/008; G01H 9/006; H04R 1/083;
H04R 1/08; H04R 7/04; H04R 2201/003

(86) International application number:
PCT/TR2019/050262

(87) International publication number:
WO 2020/214108 (22.10.2020 Gazette 2020/43)

(54) **FIBER OPTIC MEMS MICROPHONE**

FASEROPTISCHES MEMS-MIKROFON

MICROPHONE MEMS À FIBRE OPTIQUE

(84) Designated Contracting States:
AL AT BE BG CH CY CZ DE DK EE ES FI FR GB GR HR HU IE IS IT LI LT LU LV MC MK MT NL NO PL PT RO RS SE SI SK SM TR

(43) Date of publication of application:
26.01.2022 Bulletin 2022/04

(73) Proprietor: **ORTA DOGU TEKNIK UNIVERSITESI**
06800 Ankara (TR)

(72) Inventors:
- **BAYRAM, Baris**
  06800 Ankara (TR)
- **SAHİN, Asaf Behzat**
  Ankara (TR)
- **OGUZ, İlker**
  06800 Çankaya/Ankara (TR)
- **ÖZMEN, Göktug Cihan**
  06800 Çankaya/Ankara (TR)
- **KARACA, Ekin Muharrem**
  06800 Çankaya/Ankara (TR)
- **ÇAVDIR, Doga Buse**
  06800 Çankaya/Ankara (TR)

(74) Representative: **Yalçiner Patent and Consulting Ltd.**
Tunus Caddesi 85/3-4
Kavaklidere
06680 Ankara (TR)

(56) References cited:
WO-A1-2014/195372 CN-A- 101 778 328
CN-A- 104 113 813 CN-A- 109 506 764
US-B1- 6 483 619 US-B2- 7 485 847

- **DEGERTEKIN F L ET AL: "Fabrication and Characterization of a Micromachined Acoustic Sensor With Integrated Optical Readout", IEEE JOURNAL OF SELECTED TOPICS IN QUANTUM ELECTRONICS, IEEE, USA, vol. 10, no. 3, 1 May 2004 (2004-05-01), pages 643-651, XP011116315, ISSN: 1077-260X, DOI: 10.1109/JSTQE.2004.829198**
- **KARTHIK KADIRVEL et al.: "Design and Characterization of MEMS Optical Microphone for Aeroacoustic Measurement", 42nd Aerospace Sciences Meeting & Exhibit, 5- 8 January 2004 / Reno, 5 January 2004 (2004-01-05), XP055750106,**

Note: Within nine months of the publication of the mention of the grant of the European patent in the European Patent Bulletin, any person may give notice to the European Patent Office of opposition to that patent, in accordance with the Implementing Regulations. Notice of opposition shall not be deemed to have been filed until the opposition fee has been paid. (Art. 99(1) European Patent Convention).

EP 3 942 262 B1

Description

THE TECHNICAL FIELD OF THE INVENTION

5 **[0001]** The invention relates to fiber optic MEMS microphone that features electrically deflectable MEMS membrane via conversion of optical energy propagating in the optical fiber to electrical energy with photodiode chip.

PRIOR ART ABOUT THE INVENTION (PREVIOUS TECHNIC)

10 **[0002]** Microphones, which are instruments that convert sound waves into electrical signals, are being developed with MEMS technology. The MEMS microphones have become ideal for use in portable technologies with their resistance to acceleration, low energy consumption, long-term stable performance, high sensitivity and small size. MEMS fiber optic microphones are used in distributed sensor networks and hazardous industrial environments because they are resistant to electromagnetic effects. With very low loss fiber optic cables, they can be carried away for miles away. When 15 MEMS-based fiber optic microphone studies and patents in academic and industrial literature are examined, it is seen that MEMS devices are operated passively-without active voltage applied- and their sensitivities are limited and constant in operation. In commercially available microelectromechanical systems (MEMS) microphones, detection of the audible frequency range (20 Hz - 20 kHz) is utilized through some electrical measurements such as current/voltage or capacitive measurements. These measurements are vulnerable to the electrical noise of the system and the environment. In 20 addition, these microphones do not give accurate results under harsh environmental conditions such as high temperature and high pressure. Fiber optical sensors are used in a wide range of sensing applications for temperature, vibration, pressure, index of refraction sensing. Employing the microelectromechanical systems (MEMS) technology based on fiber optic sensing with extrinsic Fabry-Perot interferometry provides high sensitivity detection of high frequency ultrasound. Today, in some applications, fiber optic microphones are preferred over condenser microphones. The conventional 25 condenser microphone is a high impedance device due to the necessity of a high input impedance preamplifier for further signal processing[1]. For the condenser microphone, this additional high impedance preamplifier is an additional burden in the design which reduces the performance of the microphone even for some sophisticated electronic designs. Additionally, due to the cable capacitances, the distance between the microphone and the receiver electronics must be very small which restricts the application of the microphone in a confined space. The fiber optic MEMS microphone has very 30 high immunity to electromagnetic interference since all of the electronic components that is used in the design are kept out of the sensor probe1.The main advantage of MEMS technology is that it offers the flexibility to achieve the desired response range, bandwidth, and sensitivity by basically adjusting the size of the membrane[1,2]. Also two different methods are used with fiber optic microphones; phase and intensity modulation. Phase modulation technique gives better performance considering the measurement range and durability[2,3]. For these reasons, the necessity of finding a new way 35 of designing a MEMS microphone for audible frequency range detection has raised. It was shown that utilization of light as the way to detect sound waves gives much better performance than the microphones which senses the sound waves electrically[4].

[0003] Optical sensing technique for small displacement measurement is vital for industrial nondestructive techniques, vibration and, design and testing of microstructures for their unique advantages, such as immunity to electromagnetic 40 interferences, stability, repeatability, durability against harsh environments, high sensitivity, high resolution, and fast response[3]. The fiber optic microphone can enable innovative applications in a variety of applications due to the wide dynamic range, high sensitivity and flat frequency response over large bandwidth[1].

[0004] In the past two decades, extrinsic Fabry-Perot interferometer based pressure sensors have undergone a significant growth and substantial research has been carried out on it. Diaphragm-based extrinsic Fabry-Perot interferometer 45 sensors have been successfully used for low pressure and acoustic wave detection[5].

[0005] To obtain high fidelity Fabry-Perot interferometer based pressure sensor, the most crucial part is the MEMS membrane. The light propagating through the fiber hits the membrane at the fiber end and then reflects back. At that point, the Fabry-Perot cavity is obtained between the fiber end and the membrane. Small displacements at the membrane are detected by analyzing the interference fringes from the cavity. The feasibility of phase modulation technique is 50 experimentally proven by measurements[4].

[0006] By adjusting size of the membrane, the electrical impedance of the membrane in air can be adjusted[1]. Since both incident and reflected beams in fiber optic MEMS microphone share the same optical fiber, environmental effects at the fiber, such as changes in temperature, pressure and vibration do not significantly affect the interference signal obtained by Fabry-Perot interferometer[1]. Fiber optic microphone has the potential capability of on-line and remote 55 sensing. This type of sensor can also be extended to measure vibration and acceleration. Due to the simplicity of the structure and the ease of operation, this design can be used in variety of applications[4]. Pressure sensors can also be utilized via fiber optic idea. It is shown that linear pressure sensitivity between 0 kPa (94 dB) and 600 kPa (210 dB) is achieved in the temperature range of 20 °C - 300 °C with these pressure sensors[6].

[0007] Recently, different membrane materials, such as Parylene-C and graphene oxide, are proposed for a microphone application. Parylene-C gives strong response in the order of 2000 nm/Pa at 20 Hz. Due to the bio-compatibility of Parylene-C, these acoustic sensors are said to be very useful in biomedical applications[7]. With the developments in the fabrication of graphene oxide, reliable production of it with any desired thickness becomes possible. Graphene oxide based membrane is shown to be give flat response in 100 Hz-20 kHz ranges. It is also shown that corrugated silver membranes can be used for optical fiber microphones. Introduced corrugations on the membrane was shown to improve the performance of the microphone and the new design gives response in the order of 50 nm/Pa in the range of 63 Hz - 1 kHz[9]. In addition to the efforts of finding new membrane materials, there is ongoing research on the improvement of the shape and size of MEMS membranes. One suggested method is to microfabricate an annular corrugated MEMS membrane. In this method, the proposed design can sense the minimum detectable pressure level of 3 $\mu Pa/Hz^{1/2}$ at 1 kHz[10].

[0008] US6483619B1 discloses an optical-interference microphone having a high sensitivity and bandwidth, and that is suitable to be manufactured by micromachining techniques. The microphone includes a back member, a diaphragm and an air gap formed between the back member and diaphragm. Further, the diaphragm includes a plurality of holes. The microphone utilizes optical interference to sense the sound-induced motion of the diaphragm. A light source and detector can be included as components of the microphone or can be at a remote location and connected to the microphone with an optical fiber.

AIMS OF THE INVENTION AND A BRIEF EXPLANATION

[0009] A new approach for MEMS technology, the fiber optic MEMS microphone, is presented in this document. Our invention is a laser-powered active MEMS fiber-optic acoustic sensor microphone.

[0010] Microphones have an important place in our lives. Traditional microphones are now replaced with MEMS microphones. Small size MEMS microphones are available in capacitive and piezoelectric models.

[0011] MEMS microphones are influenced by RF and microwave signals and high magnetic fields such as MRI because they are based on capacitive or piezoelectric electrical measurement techniques.

[0012] Fiber-optic MEMS microphones are obtained by combining MEMS passive diaphragm and fiber optics. In this invention, an electrically adjustable MEMS membrane instead of a MEMS passive diaphragm is presented. Also, electrical power is generated from the incident laser light right on the spot of the MEMS membrane through a photodiode chip. In doing so, impractical electrical conduction along the fiber-optic cable is eliminted and the cost for large capacity use has been significantly reduced. At this point, the idea of transforming the energy of the light carried within the optical cable to the electrical voltage on the membrane by means of a photodetector is used.

[0013] Sensing element is the most critical part of fiber optic MEMS microphone. This sensing element, membrane, is designed such that the microphone operates in the desired range with desired sensitivity. In this invention, design and characterization of a custom-designed MEMS membrane to be used in an optical fiber optic microphone is performed which will be responsive over the audible frequency range. This design features electrically deflectable membrane having symmetrically distributed air holes across it. Microfabrication is done using a commercially available multi-user multi-project service (POLYMUMPS, MEMSCAP Inc., France). Full electrical and optical characterizations of the membrane are done using an impedance analyzer and laser vibrometer, respectively. The design includes reflective gold-coated surface which makes it suitable for optical interferometry based microphones. The transient and steady state analysis of the membrane is utilized, and the overall response of the membrane as well as the spatial response of it is obtained. The fundamental resonance of the membrane is 28 kHz which is slightly above the frequency range of interest, 20 kHz. The peak displacement of 10 nm is obtained from vibrometer measurements under 100 mV peak-to-peak voltage and 1V DC bias conditions. After converting the applied AC voltage to the pressure, the sensitivity of the membrane is calculated to be around 40 nm/Pa at 28 kHz.

[0014] The symmetry of the design is also verified through spatial analysis. This invention offers a new aspect for the design of MEMS membrane for optical microphones. This invention employs MEMS technology to realize a novel membrane rather than finding new membrane materials for fiber optic microphone applications. This MEMS membrane is designed to respond to the audible frequency range. This new design is compatible with optical sensing for detection of membrane displacement. Utilization of a mature microfabrication processes makes the design reliable and reproducible. Extensive analyses of steady state and transient responses of the membrane to different excitations are performed and the performance of the design is verified. One aspect of the invention, wherein MEMS device is respectively comprising of METAL, POLY2, POLY1, POLY0, SiN, and Si substrate from top to the bottom.

[0015] Another aspect of the invention, wherein the diameter of air holes and dimples are set to 36 μm and 12 μm.

[0016] Another aspect of the invention, wherein a photodiode chip is Ge-TIA or InGaAs P-I-N photodiode.

[0017] Another aspect of the invention, wherein value for the laser operation wavelength is 1064 nm.

[0018] Another aspect of the invention, wherein the displacement of the large perforated membrane corresponding to the sound waves in the active MEMS-based fiber optic acoustic microphone is determined by phase modulation of the light.

[0019] Another aspect of the invention, wherein the laser beam from the fiber optic cable is used both as a remote power transfer and as an acoustic signal sensor via the MEMS device.

[0020] Another aspect of the invention, wherein the control range of the MEMS membrane against acoustic stimulation and the sensitivity of the measuring system are adjusted by controlling the bias of the MEMS device in the microphone.

[0021] Another aspect of the invention, wherein to obtain sufficiently large oxide etch under the membrane, any point on the membrane must be reachable by an air hole with a maximum distance of 15 μm in-between.

[0022] Another aspect of the invention, wherein membrane on a chip carrier with gold electrical paths and gold wirebond between them.

[0023] Another aspect of the invention, wherein dimensions of the membrane design are,

- Substrate thickness (t_{subs}) is >650 μm
- Membrane diameter ($d_{membrane}$) is 1000 μm
- hole-to-hole diameter ($d_{HOLE-TO-HOLE}$) is 50 μm
- dimple diameter (d_{dimple}) is 12 μm
- hole diameter (d_{hole}) is 36 μm
- metal thickness (t_{metal}) is 0.51 μm
- POLY2 thickness (t_{poly2}) is 1.5 μm
- Dimple thickness (t_{dimple}) is 0.75 μm
- POLY1 thickness (t_{poly1}) is 2.0 μm
- POLY0 thickness (t_{poly0}) is 0.51 μm
- SiN thickness (t_{SiN}) is 0.61 μm.

[0024] Another aspect of the invention, wherein the MEMS device is remotely driven and controlled by laser power.

[0025] Another aspect of the invention, wherein the power of the laser beam is converted into a voltage source that will control the MEMS device via the photodiode integrated with the MEMS device.

THE DESCRIPTIONS OF THE FIGURE EXPLAINING THE INVENTION

[0026] The figures used to better explain fiber optic MEMS microphone developed with this invention and their descriptions are as follows:

Figure 1 A laser-powered active MEMS-based fiber-optic acoustic sensor-microphone
Figure 1a Fabry Perot interferometer measurement system
Figure 1b Photodiode supplied active MEMS fiber optic microphone structure
Figure 2 Cross-sectional view of the MEMS membrane design
Figure 3 Electrical impedance measurements of MEMS structure
Figure 3a The membrane on the chuck of the probe station as shown
Figure 3b The microscope view taken from the probe station as shown
Figure 4 Displacement measurements of MEMS structure using laser vibrometer
Figure 5 The top view of the membrane as shown
Figure 5a Polysilicon layer of the membrane with air holes
Figure 5b Zoomed view of the membrane which shows the air holes and dimples
Figure 6 Hole arrangement for optimum membrane design
Figure 7 Electrical characterization setup
Figure 8 Optical characterization setup
Figure 9 Deflection of the membrane as a function of frequency
Figure 10 Average displacement over selected area for different radial distances from the membrane
Figure 11 The analysis of the symmetry of the membrane. Response of two points that are separated by (a) 50 μm, (b) 150 μm, (c) 250 μm and (d) 350 μm from the center of the membrane
Figure 12. Spatial response of the membrane to the (a) CW inputs at 28 kHz, 51 kHz and 109 kHz (steady-state), and one cycle of sine pulses at (b) 28 kHz, (c) 51 kHz, (d) 109 kHz (transient)

THE DETAILED EXPLANATION OF THE INVENTION

[0027] The present invention has been described in detail in the following. This invention offers a new aspect for the design of MEMS membrane for optical microphones.

[0028] In this section, a novelty is going to be demonstrated.

[0029] Our invention is a laser-powered active MEMS-based fiber-optic acoustic sensor-microphone (Figure 1). The

MEMS device is integrated with an optical fiber cable end structure and a photodiode chip. A portion of the laser beam from the fiber optic cable passes back through the MEMS substrate and membrane to form a Fabry-Perot interference and go to the fiber optic interferential motion sensor. The remaining part of the incoming laser beam illuminates the photodiode chip, creating the electrical power to activate the MEMS device. By changing the laser beam power, the MEMS device is driven at different voltage values. In this way, it is possible to obtain adjustable MEMS fiber optic microphone devices with high transfer factor and dynamic response intervals. The 1064 nm value for the laser operation wavelength is chosen because this wavelength can pass the MEMS device with a low loss of silicon substrate structure and illuminate the InGaAs P-I-N photodiode that will drive the MEMS device.

[0030] MEMS membrane, Laser diode, photodiode Ge-TIA and optical fiber circulator are shown in figure 1a. Laser diode which is shown in Figure 1a as a 1064 nm value. MEMS membrane, photodiode, reflected laser light, incident laser light and Optical fiber are shown in 1b. Optical fiber which is shown in Figure 1b as a Φ125 μm and Φ425 μm.

[0031] MEMS fiber optic microphones have a vibrating diaphragm that corresponds to the acoustic sound wave. This diaphragm is not in any way an electrically controllable structure, i.e. it is passive. The diaphragm resonance frequencies are constant. With the fiber optic cable, the intensity or phase modulation of the incoming light is determined by the displacement of the diaphragm corresponding to the sound wave. In general, different materials of the diaphragm structure or diaphragm surface corrugation shapes are tried to increase sensitivity.

[0032] In our invention, the displacement of the large perforated membrane (Figure 2) corresponding to the sound waves in the active MEMS-based fiber optic acoustic microphone is determined by phase modulation of the light. This allows the membrane to adjust its sensitivity to sound waves.

1) The MEMS device is remotely driven and controlled by laser power. The laser beam from the fiber optic cable is used both as a remote power transfer and as an acoustic signal sensor via the MEMS device.The power of the laser beam is converted into a voltage source that will control the MEMS device via the photodiode integrated with the MEMS device. In the literature, a MEMS study activated by laser power was not found.

2) In the active MEMS-based fiber-optic acoustic sensor, the control range of the MEMS membrane against acoustic stimulation and the sensitivity of the measuring system are adjusted by controlling the bias of the MEMS device in the microphone. This results in a wider dynamic response range than conventional MEMS fiber optic microphones. In the literature research, no MEMS fiber optic microphone working with active power supply has been found.

3) The MEMS device is integrated with an optical fiber cable end structure and a photodiode chip. The laser beam from the fiber optic cable will be used both as a remote power transfer and as an acoustic signal sensor via the MEMS device. A study using laser beam for remote power transfer in a sensor system has not been found in the literature.

[0033] Light is used not only for displacement, but also for energy transmission. The presence of an active membrane in which we can adjust the resonance frequency during use with this energy transmission is particularly important for microphones operating in a very wide frequency range (20 Hz to 20,000 Hz).

[0034] Membrane of a fiber-optic MEMS microphone is the sensing element of it. The design of membrane concerns several issues such as the reproducibility, durability, stable performance of the membrane. These issues are addressed to the microfabrication process. Based on commercially available multi-user multi-processes (MUMPS) offered by foundries, POLYMUMPS process (MEMSCAP Inc., France) is selected due to its suitability for microfabrication of airborne membranes supported by the non-limiting process design rules for our intended microphone application. Furthermore, reproducibility and consistency of this mature process is considered to be advantageous for the realization of high fidelity membrane, which is of utmost importance for the optical phase detection of light.

[0035] This process is based on polysilicon layers. The ability to design membranes and the ability to etch sacrificial oxide layers under the polysilicon layers makes this process valuable for our design. Obtain perfect etching of sacrificial oxide layers requires placement of holes in the polysilicon layers. The distance between any etching holes cannot be larger than 30 μm. In our design, we also take into account the process variations in the design of our membrane. On top of the membrane, we put metal layer for the reflection of light from the membrane. CO_2 dry etch in addition to the standard HF wet etch for oxide removal is used. CO_2 dry is used to prevent the stiction of the adhesion between the membrane and the substrate for the large aspect ratio used in the membrane (1:500). Very low compressive stress (< 7 MPa) of POLY2 membrane material with a thickness of 2 μm and very low tensile stress (<24 MPa) of METAL coverage of 0.51 μm on the membrane results in an almost ideal compensation of stress resulting an equivalent stress less than 1 MPa[11]. This makes our large aspect-ratio membrane having negligible curvature due to residual stress.

[0036] The diameter of the membrane is adjusted to obtain high response in the audible frequency range. The formula given by Equation 1 is used[12]. This formula gives the first resonance frequency of a circular membrane by taking the membrane material properties and the membrane dimensions into account. For this design, the material properties and

required dimensions are taken from the MEMSCAP.[12]

$$f \cong \frac{20.42}{\pi a^2}\sqrt{\frac{D}{h\rho}} \quad , D = \frac{Eh^3}{12(1-\mu^2)} \qquad (1)$$

where *a* is the diameter, *h* is the thickness, ρ is the mass density, which is taken as 2330 kg/m^3, E is the Young's Modulus, which is taken as 169 GPa, and μ is the Poisson's ratio, which is taken as 0.22, of the membrane.

[0037] Since the detection of audible signals in 20 Hz - 20 kHz frequency band is desired, the resonance frequency that is slightly above the upper limit of this band is required.

[0038] The resultant design of the membrane consists of a polysilicon membrane with air holes and it is called as a meshed-structured membrane. The top view of the membrane is shown in Fig. 5.

[0039] The diameter of air holes and dimples are set to 36 μm and 12μm, respectively. The distance between the centers of two air holes is determined according to the design rules. To obtain sufficiently large oxide etch under the membrane, any point on the membrane must be reachable by an air hole with a maximum distance of 15μm in-between by design rules. The geometric problem that is solved is represented in Fig. 6.

[0040] The design is fully symmetric, and the holes and their separations are identical in both directions on the membrane. There are two variables in this design, the diameter of the holes and the distance between the centers of the holes. Since the placement of holes is fully symmetric, an equilateral triangle is obtained with the corners taken as any three air hole centers. After calculations, it is found that $2d_{HOLE-TO-HOLE} - \sqrt{3}d_{HOLE} \lessapprox 30\sqrt{3}\mu m$. Another objective is to maximize the fill factor. Fill factor (FF) of the design is given as $FF = 1 - \frac{\pi}{2\sqrt{3}}(\frac{d_{HOLE}}{d_{HOLE-TO-HOLE}})^2$. Since the amount of the light reflected from the membrane should be sufficiently large for the detection of the displacement of the membrane, at least 50% fill factor is aimed. Therefore, the constraint becomes $\frac{d_{HOLE}}{d_{HOLE-TO-HOLE}} < 0.75$. To optimize both constraints, D_{HOLE} = 36 μm and $d_{HOLE\text{-}TO\text{-}HOLE}$ = 50 μm are chosen with safety margins. In this case, the fill factor becomes 53% and hole-to-hole distance becomes 50 μm. The maximum distance between any point on the membrane and the air hole is 14 μm.

[0041] The cross-sectional view of the resultant is shown in Fig. 2 and the values of the parameters in this figure are given in Table I.

Table I. Values of the representative dimensions of the design.

Dimension parameter	Value
Membrane diameter ($d_{MEMBRANE}$), μm	1000
Support length ($d_{SUPPORT}$), μm	150
Hole-to-hole diameter ($d_{HOLE\text{-}TO\text{-}HOLE}$), μm	50
Dimple diameter (d_{DIMPLE}), μm	12
Hole diameter (d_{HOLE}), μm	36
Metal thickness (t_{METAL}), μm	0.51
POLY2 thickness (t_{POLY2}), μm	1.5
Dimple thickness (t_{DIMPLE}), μm	0.75
POLY1 thickness (t_{POLY1}), μm	2.0
POLY0 thickness (t_{POLY0}), μm	0.51
SiN thickness (t_{SiN}), μm	0.61
Substrate thickness (t_{SUBS}), μm	>650

ELECTRICAL AND OPTICAL MEASUREMENT SETUP

[0042] To characterize and verify the performance of the microfabricated MEMS membrane, electrical impedance and

optical laser vibrometer measurements are employed. Cumulative response of the whole membrane is achieved via electrical whereas spatial response of spots as small as 2 μm can be collected via optical measurements. To characterize the membrane electrically, network and impedance analyzer (5061B, Keysight Technologies, California, USA) and triax connected probe station (EPS150X, Cascade MicroTech, Oregon, USA) are used as shown in Fig. 7. Series Gain-Phase mode using LF-Out port is used.

[0043] In this setup, membrane is placed on the chuck of the probe station. Electrical connections from ground and signal pads of the MEMS chip are made using tungsten needles (PTT-120-/4-25, Cascade MicroTech, Oregon, USA) followed by triax-to-BNC adapter to network and impedance analyzer. A power splitter (Agilent 11667L) is used to connect the device to the network analyzer properly to implement the suggested configuration of low frequency measurement of high impedance device.

[0044] The series capacitance (C_s) and series resistance (R_s) measurements are taken to detect any resonance frequency in the frequency range of 1 kHz-100 kHz. During measurements Intermediate Frequency Band Width (IFBW) is set to 500Hz with an averaging of 32. 10dBm ($1V_{peak\text{-}to\text{-}peak}$) sinusoidal signal is used and 1601 data points are taken in the given frequency range. DC voltage is changed from 0 V up to 3 V.

[0045] Optical characterization is done with the setup as shown in Fig. 8. Laser Vibrometer (OFV5000, Polytec, Germany) is used together with the digital oscilloscope (DSO6014A, Agilent, California, USA), the function generator (33250A, Agilent, California, USA) and a personal computer with LabView (National Instruments, Texas, USA) on it to control the devices in the setup.

[0046] Optical characterization is based on the detection of the displacement of the MEMS membrane as a result of the electrical excitation. A laser light at 633 nm wavelength is sent to the membrane and the reflected light is used to understand the deflection of the membrane via the interferometer that is utilized between the membrane and the laser light. In fact, this way of displacement measurement is very similar to the way that is used in fiber optic microphones.

[0047] To generate an acoustical pressure on the membrane, the electrical excitation is done by a function generator which generates 0.1 V peak-to-peak sinusoidal signal with a DC bias voltage of 1 V. The excitation frequency is swept from 3 kHz to 150 kHz. Besides the general response of the membrane, this optical characterization setup enables the spatial inspection of the membrane. In other words, by directing the laser light on different points on the membrane, spatial response of the membrane to any excitation can also be obtained.

RESULTS

[0048] The electrical characterization setup is prepared by putting the membrane on the chuck of the probe station as shown in Fig. 3 (a). By using needles, electrical connections are utilized. The microscope view taken from the probe station is as shown in Fig. 3 (b).

[0049] To avoid the collapse of the membrane on the ground plate, maximum of 3V DC bias is applied between the plates of the microphone. The measured C_s and R_s values are shown in Fig. 3. Two resonance frequencies are observed at 30 kHz and 56 kHz, respectively.

[0050] In optical measurement setup, the membrane is placed in a chip carrier as shown in Fig. 4 (b) and the electrical pads are connected to electrically conductive gold lines on the chip carrier by gold wire bonds as shown in Fig. 4 (b). Chip carrier has two SMA (SubMiniature version A) connectors which are used to excite the membrane electrically through its pads. The signal generator is connected to the MEMS device and it is also connected to the oscilloscope as a triggering signal for the output of the vibrometer.

[0051] In the optical measurement, all data were taken from 21 points on the membrane to understand its overall response as well as its spatial response. Those 21 points are 50 μm apart from each other with the 11th point at the center of the membrane as shown in Fig. 4(a). Input frequency is swept from 3 kHz to 150 kHz with a continuous wave (CW) sinusoidal excitation. The response of the membrane in both spatial and frequency domains are shown in Fig. 4 (b). It is observed that there are three resonance frequencies at 28 kHz, 51 kHz and 109 kHz. Region around the center of the membrane gives the highest response to any input.

[0052] Total response of the membrane considering the amount of deflection is also obtained by processing the spatial data. The overall response and the response of the central point are shown in Fig. 9. At 28 kHz, the average displacement of the membrane is 5 nm in average and 10nm in the center. The fractional 3-dB bandwidth of this resonance is 32 %.

[0053] To determine where to focus the laser light to obtain the maximum deflection per area the responses of data points at 28 kHz are analyzed. Average displacement over selected area is obtained for different radial distances from the center of the membrane and the resultant characteristics is shown in Fig. 10. The optimum area to focus the light has a radius of 150μm. The average displacement is almost constant for circular areas with radius ranging from 50 μm to 250 μm.

[0054] To analyze the symmetry in the response of the membrane, the data from the points that are 50 μm, 150 μm, 250 μm and 350 μm distant from the center of the membrane are used. This characteristics is shown in Fig. 11.

[0055] For the points that are 50 μm distant from the center of the membrane, it is realized that their peak responses

are at the same frequencies. This situation occurs also for 100 μm distant points. For 250 μm distant points, the location of the second resonance frequency changes slightly by 3.8 %. Further small deviations are observed for 350 μm distant points. The first, second and third resonance frequencies change by 3.6 %, 5.9 % and 4 %, respectively.

[0056] The spatial steady state responses of the membrane to the input signals at 28 kHz, 51 kHz and 109 kHz are shown in Fig. 12 (a). To obtain the temporal transient response of the membrane, single cycle sinusoidal signals at the resonance frequencies, 28 kHz, 51 kHz and 109 kHz are used. The responses are as shown in Fig. 12 (b-d). It is observed that the transient response of the membrane to the input at 28 kHz has longest ringing response. All of the transient responses decay with time.

[0057] Electrical characterization is applicable to the membrane since it can be modelled as a series capacitor and a series resistor. A parallel plate capacitor can be visualized by considering the membrane and the substrate as parallel plates. In the design of the microphone, a 450μm-radius, 0.5pm-thick polysilicon layer is added on the substrate which is just below the membrane by 2 μm. This part is called the ground plate and it is connected to the ground pads by polysilicon lines. The movable membrane is also connected to the signal pads via polysilicon lines.

[0058] From electrical measurements as shown in Fig. 3, first resonance frequency at 30 kHz is close to the expected one which was calculated from the Equation (1) as 26 kHz. From series capacitance data, it is observed that this frequency changes from 29.4 kHz to 30.6 kHz when the applied DC voltage is changed from 0V to 3V. The resonance frequency is observed around 56 kHz and it changes by 3 kHz with the applied DC voltage. Therefore, the resonance frequency of the membrane is fine tunable with the applied DC voltage. From 0V to 2V, the first resonance frequency increases by 750 Hz which may be due to the stress stiffening and from 0V to 3V, it decreases by 250 Hz which may be due to the effect of spring softening dominating stress stiffening[14].

[0059] The measured capacitance values in Fig. 3 (a) are not actual capacitance values of the MEMS membrane, which is theoretically calculated to be 1.4 pF, due to the effects of cabling and lack of calibration at the end of probes. They only show the existence of resonance frequencies, and high capacitance values indicate that the resonances around 30 kHz and 56 kHz are strong. The measured resistance values are relatively high due to the resistive lightly-doped polysilicon lines compared to the highly conductive metal.

[0060] Modal shapes of the resonances are shown in Fig. 4 (b). It can be observed that the first resonance frequency is the fundamental resonance frequency since it has no nulls in its mode shape. The second resonance frequency at 51 kHz and the third resonance frequency at 109 kHz has one and two nulls along the radial direction as expected, respectively. This data supports that these are the first three resonances of the membrane.

[0061] In addition to the operation of the device around 28 kHz, from Fig. 4. (b), this membrane can be used to operate at 58 kHz and 109 kHz. By focusing the light on circular areas with 150 μm and 100 μm radius, this membrane can operate at 58 kHz and 109 kHz, respectively.

[0062] If the parallel plate capacitor assumption is used, the applied voltage can be used to model the force acting on the plates of the capacitor, namely the membrane. This information is valuable since the membrane is required to respond sound pressure. From the average displacement data in Fig. 9, this calculation is done by $P = \frac{1}{2}\varepsilon E^2 = \frac{1}{2}\varepsilon(\frac{V}{d_{eff}})^2$ formula which represents the amount of pressure that acts on the plates of a parallel plate capacitor. In this formula, ε is actually ε_0, which is the permittivity of free space, and gap between the plates and 1.25 μm for the regions with dimples. First, the gap between the plates should be calculated. For a parallel plate capacitor, deflection of the plate as a function of applied voltage is given as $V_n{}^2 = \frac{27}{4}x_n(1-x_n)^2$, where $V_n = \frac{V}{V_{collapse}}$, $V_{collapse}$ being the collapse voltage of the membrane, $x_n = \frac{x}{d_{eff}}$, d_{eff} being the effective gap between the plates of the capacitors[13]. In this design, $V_{collapse}$ is observed to be larger than 3V. d_{eff} can be calculated from different regions of the membrane, namely the polysilicon region with dimples, region-1 and the polysilicon regions without dimples, region-2. The air gap of region-1 is g_1 = 1.25 μm and the air gap of region-2 is g_1 = 2 μm. Effective gap can be calculated by $\frac{1}{9}(\frac{1}{g_1})^2 + (\frac{1}{g_2})^2 = \frac{10}{9}(\frac{1}{d_{eff}})^2$ resulting in d_{eff} being 1.86 μm. If we insert this value into the equation, we can find that for 1V DC bias, as in the optical measurement setup, x_n = 0.01 which results in x = 18.6 nm. Since this value is negligible compared to d_{eff} =1.86 μm, it can be ignored. The applied voltage is the sum of DC and ac voltages as $V = V_{DC} + v_{ac}\cos(wt)$. By taking square of it, we obtain three terms: the purely DC term, which is already responsible for the change of the effective gap between the plates, the ac term with frequency two times the excitation frequency, which is neglected and the ac term with frequency same as the excitation frequency. This final term should be used in the pressure formula. By taking d_{eff} = 1.86μ*m*, it is found that the average displacement per pressure of the membrane at 28 kHz is approximately 40 nm/Pa. Highly reflective surface

and high pressure sensitivity of the membrane make it suitable for microphone applications. The average displacement of the membrane is predicted to be increase with the larger DC bias voltages. Therefore, operating this device around 3V DC bias gives the highest response and this makes the detection of the displacement easier.

[0063] The area that the laser light to be spotted is important since width of the light beam increases with distance. The amount of power that is coupled to the fiber after reflection starts decreasing after the critical width of the beam which is equal to the diameter of the fiber. By taking the distance light travels constant, the only parameter to change is the width of the beam when it hits the membrane. This width should be large enough to obtain the sufficient amount of deflection information from the membrane. From Fig. 10, the optimum width is calculated as 300 μm (150μm-radiues circle). Therefore, focusing light to the area with 150 μm radius would be the best solution considering both the sensitivity and the amount of light that couples back to the fiber.

[0064] The membrane shows a highly symmetric response within the area with radius 250 μm as shown in Fig. 11. The symmetry can also be verified from the transient response of the membrane to the one cycle sinusoidal excitations as shown in Fig. 12 (b),(c),(d). From symmetry property, the central operation of the membrane is verified; the membrane has circular symmetry with respect to the center of it.

[0065] The characteristics of a custom designed 1300μm×1300μm featuring 1.5 μm-thick, 1000 μm-diameter MEMS membrane with 36 μm-diameter air holes which is designed as the sensing element for a fiber optic microphone is microfabricated by POLYMUMPS process and its characteristics are investigated. Air holes are used in the design to obtain sacrificial etch of oxide layers under the membrane. These holes are designed such that the fill factor of the design is 53 %. The surface of the membrane is gold-coated which utilizes a reflective surface for the light. The resonance frequencies of the design are obtained by electrical and optical measurement setups. The fundamental resonance frequency of the design changed by 3 % with the change of the applied dc voltage from 0V to 3V. Higher order modes are also observed and the center of the membrane gives strong response also to the higher modes. The response of the design is spatially symmetric and the mode shapes suggests that the resonance at 28 kHz is the fundamental mode of the membrane. By obtaining the resonance frequency slightly above the audible frequency range, strong response and almost no phase reversal have achieved. High sensitivity of the design, 40 nm/Pa, makes it suitable for fiber optic microphones. High circular symmetry of the membrane is also important due to the circular spots of laser lights. This design also offers the flexibility of selecting the area to focus light on the membrane since it gives almost the same response within the 250 μm-radius area. By the characteristics of the membrane, this design is verified to be suitable for fiber optic microphones.

[0066] From the above detailed description, a fiber optic MEMS microphone is claimed, according to claim 1.

References

[0067]

[1]Chonghua Zhou, Stephen V. Letcher, and Arun Shukla, "Fiber-optic microphone based on a combination of Fabry-Perot interferometry and intensity modulation", The J. Acoust. Soc. Am., 98, 1042 (1995).

[2]Ming Li, Ming Wang,"Optical MEMS pressure sensor based on Fabry-Perot interferometry", Optics Express, Vol. 14, No.4 (2006).

[3]Ji-Huan Chen, Xu-Guang Huang, Jia-Rong Zhao, Jin Tao, Wei-Xin He, Song-Hao Liu, "Fabry-Perot interference-based fiber-optic sensor for small displacement measurement", Optics Communications 283, 3315-3319 (2010).

[4]J. A. Bucaro, H. D. Dardy, and E. F. Carome, "Fiber-optic hydrophone", J. Acoust. Soc. Am., 62, 1302 (1998).

[5]Qingxu YU and Xinlei ZHOU, "Pressure Sensor Based on the Fiber-Optic Extrinsic Fabry-Perot Interferometer",Photonic Sensors Vol. 1, No. 1: 72-83 (2011).

[6]G.C Fanga, P.G Jia, Q. Caoa, and J.J Xiong, "MEMS Fiber-optic Fabry-Perot pressure sensor for high temperature application", Proc. of SPIE Vol. 10155, 101552H (2016).

[7]Zhenfeng Gong, Ke Chen, Xinlei Zhou, Yang Yang, Zhihao Zhao, Helin Zou, and Qingxu Yu, "High Sensitivity Fabry-Perot Interferometric Acoustic Sensor for Low-Frequency Acoutic Pressure Detections", J. Lightwave Tech., Vol. 35, No. 24 (2017).

[8]Yu Wu, Caibin Yu, Fan Wu, Chen Li, Jinhao Zhou, Yuan Gong, Yunjiang Rao, Yuanfu Chen, "A Highly Sensitive Fiber-Optic Microphone Based on Graphene Oxide Membrane", J. Lightwave Tech., Vol. 35, No. 19 (2017).

[9]Bin Liu, Han Zhou, Lei Liu, Xing Wang, Mingguang Shan, Peng Jin, Zhi Zhong, "An Optical Fiber Fabry-Perot Microphone Based on Corrugated Silver Diaphragm", IEEE Transactions on Instrumentation and Measurement, Vol. 67, No. 8 (2018).

[10]Xueqi Lu, Yu Wu, Yuan Gong, Yunjiang Rao, "A miniature fiber-optic microphone based on annular corrugated MEMS diaphragm", J. Lightwave Tech., doi: 10.1109/JLT.2018.2868964 (2018).

[11]Steve T. Cho, Khalil Najafi, Kensall D. Wise, "Internal Stress Compensation and Scaling in Ultrasensitive Silicon Pressure Sensor", IEEE Transaction on Electron Devices Vol. 39, No.4 (1992).

[12]M. Giovanni, Flat and Corrugated Diaphragm Design Hand-book (1982).

[13]G. G. Yaralioglu, A. S. Ergun, B. Bayram, E. Haeggstrom and B. T. Khuri-Yakub, "Calculation and measurement of electromechanical coupling coefficient of capacitive micromachined ultrasonic transducers,", IEEE Transactions on Ultrasonics, Ferroelectrics, and Frequency Control, vol. 50, no. 4, pp. 449-456, (2003).

[14]I. O. Wygant, M. Kupnik and B. T. Khuri-Yakub, "Analytically calculating membrane displacement and the equivalent circuit model of a circular CMUT cell,", IEEE Ultrasonics Symposium, Beijing, 2008, pp. 2111-2114,(2008).

Claims

1. A fiber optic MEMS microphone, comprising;

    - An optical fiber cable,
    - A MEMS device integrated at the end of the optical fiber cable, wherein the MEMS device features a membrane coated with optically reflective material that reflects an incident laser light and comprising air holes that transmit the incident laser light;
    - A photodiode chip placed on top of the MEMS device and electrically wired to the SIGNAL and GND pads of the MEMS device, for biasing the MEMS device;
    - A laser diode for providing a power adjustable laser light beam;

    wherein the MEMS device is capable of reflecting part of the incident laser light from the membrane back to the optical fiber, for detection of the membrane displacement via phase modulation or intensity modulation of the incident laser light, whereas allowing the remaining part of the incident laser light to be transmitted through the membrane onto the photodiode chip, for the generation of voltage across the photodiode chip, wherein the MEMS device is thus adapted to be biased at different voltage values by adjusting the laser light beam power.

2. The fiber optic MEMS microphone according to claim 1; wherein MEMS device comprises a metal layer, a first polysilicon layer (POLY2), a second polysilicon layer (POLY1), a third polysilicon layer (POLYO), a SiN layer and a Si substrate from top to the bottom.

3. The fiber optic MEMS microphone according to claim 1; wherein the membrane comprises dimples, and the diameter of the air holes and the dimples are set to 36 μm and 12 μm.

4. The fiber optic MEMS microphone according to claim 1; wherein the photodiode chip is Ge-TIA or InGaAs P-I-N photodiode.

5. The fiber optic MEMS microphone according to claim 1; wherein value for the laser operation wavelength is 1064 nm.

6. The fiber optic MEMS microphone according to claim 1; wherein the displacement of the membrane corresponding to sound waves is determined by phase modulation of the light.

7. The fiber optic MEMS microphone according to claim 1; wherein the laser light beam from the fiber optic cable is used both as a remote power transfer and for sensing an acoustic signal via the MEMS device.

8. The fiber optic MEMS microphone according to claim 1; wherein a the control range of the membrane against acoustic stimulation and a the sensitivity of the measuring system are adjusted by controlling the bias of the MEMS

device in the microphone.

9. The fiber optic MEMS microphone according to claim 1; wherein to obtain sufficiently large oxide etch under the membrane, any point on the membrane must be reachable by an air hole with a maximum distance of 15 μm in-between.

10. The fiber optic MEMS microphone according to claim 1; wherein the membrane is placed on a chip carrier with gold electrical paths and gold wirebond between them.

11. The fiber optic MEMS microphone according to claim 1; wherein dimensions of the membrane design are,

• Substrate thickness (t_{subs}) is >650 μm
• Membrane diameter ($d_{membrane}$) is 1000 μm
• hole-to-hole diameter ($d_{HOLE-TO-HOLE}$) is 50 μm
• dimple diameter (d_{dimple}) is 12 μm
• hole diameter (d_{hole}) is 36 μm
• metal thickness (t_{metal}) is 0.51 μm
• POLY2 thickness (t_{poly2}) is 1.5 μm
• Dimple thickness (t_{dimple}) is 0.75 μm
• POLY1 thickness (t_{poly1}) is 2.0 μm
• POLY0 thickness (t_{poly0}) is 0.51 μm
• SiN thickness (t_{SiN}) is 0.61 μm.

12. The fiber optic MEMS microphone according to claim 1; wherein the MEMS device is remotely driven and controlled by the laser light beam power.

13. The fiber optic MEMS microphone according to claim 1; wherein the power of the laser beam is converted into a voltage source that will control the MEMS device via the photodiode placed on top of the MEMS device.

Patentansprüche

1. Faseroptisches MEMS-Mikrofon, umfassend;

• Ein optisches Faserkabel,
• Eine MEMS-Vorrichtung, das am Ende des optisches Faserkabels integriert ist, wobei die MEMS-Vorrichtung eine Membran aufweist, die mit einem optisch reflektierenden Material beschichtet ist, das ein einfallendes Laserlicht reflektiert und Luftlöcher umfasst, die das einfallende Laserlicht durchlassen;
• Ein Fotodiodenchip, der auf der MEMS-Vorrichtung platziert und elektrisch mit den SIGNAL- und GND-Pads der MEMS-Vorrichtung verdrahtet ist, um die MEMS-Vorrichtung vorzuspannen;
• Eine Laserdiode zur Bereitstellung eines leistungseinstellbaren Laserlichtstrahls;

wobei die MEMS-Vorrichtung geeignet ist, einen Teil des einfallenden Laserlichts von der Membran zurück zur optischen Faser zu reflektieren, um die Membranverschiebung durch Phasenmodulation oder Intensitätsmodulation des einfallenden Laserlichts zu erfassen, während der verbleibende Teil des einfallenden Laserlichts durch die Membran auf den Fotodiodenchip übertragen werden kann, um eine Spannung über dem Fotodiodenchip zu erzeugen, wobei die MEMS-Vorrichtung somit dazu angepasst ist, bei unterschiedlichen Spannungswerten durch Anpassung der Laserlichtstrahlleistung vorgespannt zu werden.

2. Faseroptisches MEMS-Mikrofon nach Anspruch 1; wobei die MEMS-Vorrichtung eine Metallschicht, eine erste Polysiliziumschicht (POLY2), eine zweite Polysiliziumschicht (POLY1), eine dritte Polysiliziumschicht (POLYO), eine SiN-Schicht und ein Si-Substrat von oben nach unten umfasst.

3. Faseroptisches MEMS-Mikrofon nach Anspruch 1; wobei die Membran Vertiefungen aufweist und der Durchmesser der Luftlöcher und der Vertiefungen auf 36 μm und 12 μm eingestellt ist.

4. Faseroptisches MEMS-Mikrofon nach Anspruch 1; wobei der Photodiodenchip eine Ge-TIA- oder InGaAs-P-I-N-Photodiode ist.

5. Faseroptisches MEMS-Mikrofon nach Anspruch 1; wobei der Wert für die Laserbetriebswellenlänge 1064 nm beträgt.

6. Faseroptisches MEMS-Mikrofon nach Anspruch 1; wobei die Verschiebung der den Schallwellen entsprechenden Membran durch die Phasenmodulation des Lichts bestimmt wird.

7. Faseroptisches MEMS-Mikrofon nach Anspruch 1; wobei der Laserlichtstrahl aus dem faseroptischen Kabel sowohl zur Fernübertragung von Energie als auch zur Erfassung eines akustischen Signals über die MEMS-Vorrichtung verwendet wird.

8. Faseroptisches MEMS-Mikrofon nach Anspruch 1; wobei ein Kontrollbereich der Membran gegen akustische Stimulation und eine Empfindlichkeit des Messsystems durch Steuerung der Vorspannung der MEMS-Vorrichtung im Mikrofon eingestellt werden.

9. Faseroptisches MEMS-Mikrofon nach Anspruch 1; wobei zur Erhaltung einer ausreichend großen Oxidätzung unter der Membran jeder Punkt auf der Membran durch ein Luftloch mit einem maximalen Abstand von 15 μm dazwischen erreichbar sein muss.

10. Faseroptisches MEMS-Mikrofon nach Anspruch 1; wobei die Membran auf einem Chipträger mit elektrischen Goldpfaden und Golddrahtverbindung zwischen diesen Pfaden platziert ist.

11. Faseroptisches MEMS-Mikrofon nach Anspruch 1; wobei die Abmessungen des Membrandesigns wie folgt sind,

• Die Substratdicke (t_{Subs}) ist >650 μm
• Der Membrandurchmesser ($d_{Membran}$) ist 1000 μm
• Der Loch-zu-Loch-Durchmesser ($d_{LOCH-ZU-LOCH}$) ist 50 μm
• Der Vertiefungsdurchmesser ($d_{Vertiefung}$) ist 12 μm
• Der Lochdurchmesser (d_{Loch}) ist 36 μm
• Die Metalldicke (t_{Metall}) ist 0.51 μm
• Die POLY2-Dicke (t_{poly2}) ist 1.5 μm
• Die Vertiefungsdicke ($t_{Vertiefung}$) ist 0.75 μm
• Die POLY1-Dicke (t_{poly1}) ist 2.0 μm
• Die POLYO-Dicke (t_{poly0}) ist 0.51 μm
• Die SiN-Dicke (t_{SiN}) ist 0.61 μm.

12. Faseroptisches MEMS-Mikrofon nach Anspruch 1; wobei die MEMS-Vorrichtung durch die Leistung des Laserlichtstrahls aus der Ferne angetrieben und gesteuert wird.

13. Faseroptisches MEMS-Mikrofon nach Anspruch 1; wobei die Leistung des Laserstrahls in eine Spannungsquelle umgewandelt wird, die die MEMS-Vorrichtung über die oben auf der MEMS-Vorrichtung platzierte Fotodiode steuern wird.

Revendications

1. Microphone MEMS à fibres optiques, comprenant ;

• Un câble à fibres optiques,
• Un dispositif MEMS intégré à l'extrémité du câble à fibres optiques, dans lequel le dispositif MEMS comporte une membrane recouverte d'un matériau optiquement réfléchissant qui reflète une lumière laser incidente et comprend des trous d'air qui transmettent la lumière laser incidente ;
• Une puce photodiode placée au-dessus du dispositif MEMS et connectée électriquement aux plots SIGNAL et GND du dispositif MEMS, pour solliciter le dispositif MEMS ;
• Une diode laser pour fournir un faisceau de lumière laser à puissance réglable ; dans lequel le dispositif MEMS est capable de réfléchir une partie de la lumière laser incidente de la membrane vers la fibre optique, pour détecter le déplacement de la membrane par modulation de phase ou modulation d'intensité de la lumière laser incidente, tout en permettant à la partie restante de la lumière laser incidente d'être transmise à travers la membrane sur la puce photodiode, pour la génération d'une tension à travers la puce photodiode, dans lequel le dispositif MEMS est ainsi adapté pour être sollicité à différentes valeurs de tension en ajustant la puissance

du faisceau de lumière laser.

2. Microphone MEMS à fibres optiques selon la revendication 1 ; dans lequel le dispositif MEMS comprend une couche métallique, une première couche de polysilicium (POLY2), une deuxième couche de polysilicium (POLY1), une troisième couche de polysilicium (POLYO), une couche de SiN et un substrat de Si de haut en bas.

3. Microphone MEMS à fibres optiques selon la revendication 1 ; dans lequel la membrane comprend des alvéoles, et le diamètre des trous d'air et des alvéoles sont mis à 36 μm et 12 μm.

4. Microphone MEMS à fibres optiques selon la revendication 1; dans lequel la puce photodiode est une photodiode Ge-TIA ou InGaAs P-I-N.

5. Microphone MEMS à fibres optiques selon la revendication 1 ; dans lequel la valeur de la longueur d'onde de fonctionnement du laser est de 1064 nm.

6. Microphone MEMS à fibres optiques selon la revendication 1 ; dans lequel le déplacement de la membrane correspondant aux ondes sonores est déterminé par la modulation de phase de la lumière.

7. Microphone MEMS à fibres optiques selon la revendication 1 ; dans lequel le faisceau de lumière laser provenant du câble à fibres optiques est utilisé à la fois comme transfert d'énergie à distance et pour la détection d'un signal acoustique par le dispositif MEMS.

8. Microphone MEMS à fibres optiques selon la revendication 1 ; dans lequel une plage de contrôle de la membrane contre la stimulation acoustique et une sensibilité du système de mesure sont réglées en contrôlant la sollicitation du dispositif MEMS dans le microphone.

9. Microphone MEMS à fibres optiques selon la revendication 1 ; dans lequel pour obtenir une gravure d'oxyde suffisamment importante sous la membrane, tout point sur la membrane doit être accessible par un trou d'air avec une distance maximale de 15 μm entre les deux.

10. Microphone MEMS à fibres optiques selon la revendication 1 ; dans lequel la membrane est placée sur un support de puce avec des chemins électriques en or et des fils d'or entre eux.

11. Microphone MEMS à fibres optiques selon la revendication 1 ; dans lequel les dimensions de la conception de la membrane sont les suivantes,

- l'épaisseur du substrat (t_{subs}) est >650 μm
- le diamètre de la membrane ($d_{membrane}$) est de 1000 μm.
- le diamètre de trou à trou ($d_{TROU\text{-}À\text{-}TROU}$) est de 50 μm
- le diamètre de l'alvéole ($d_{alvéole}$) est de 12 μm
- le diamètre du trou (d_{trou}) est de 36 μm
- l'épaisseur du métal ($t_{métal}$) est de 0.51 μm
- l'épaisseur du POLY2 (t_{poly2}) est de 1.5 μm.
- l'épaisseur de l'alvéole ($t_{alvéole}$) est de 0.75 μm.
- l'épaisseur de POLY1 (t_{poly1}) est de 2.0 μm.
- l'épaisseur du POLYO (t_{poly0}) est de 0.51 μm.
- l'épaisseur de SiN (t_{SiN}) est de 0.61 μm.

12. Microphone MEMS à fibres optiques selon la revendication 1 ; dans lequel le dispositif MEMS est piloté et contrôlé à distance par la puissance du faisceau de lumière laser.

13. Microphone MEMS à fibres optiques selon la revendication 1 ; dans lequel la puissance du faisceau laser est convertie en une source de tension qui contrôlera le dispositif MEMS par la photodiode placée au sommet du dispositif MEMS.

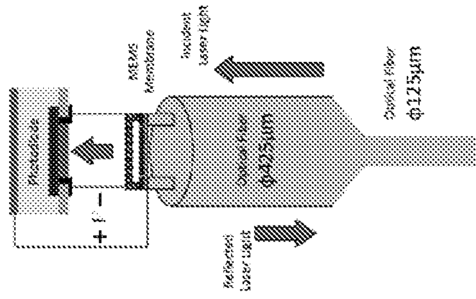

Figure 1b

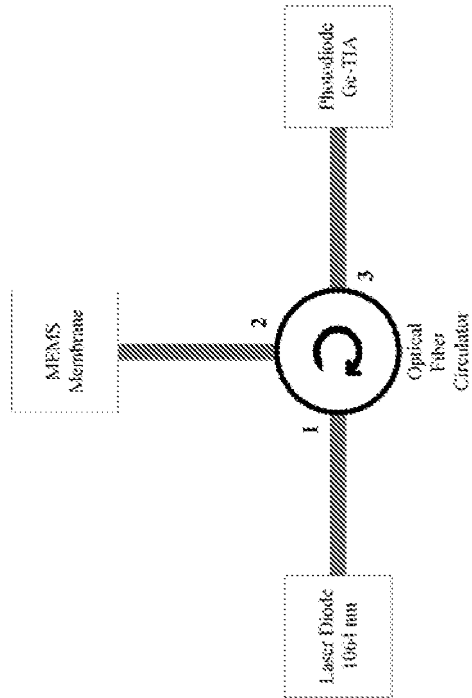

Figure 1a

Figure 1

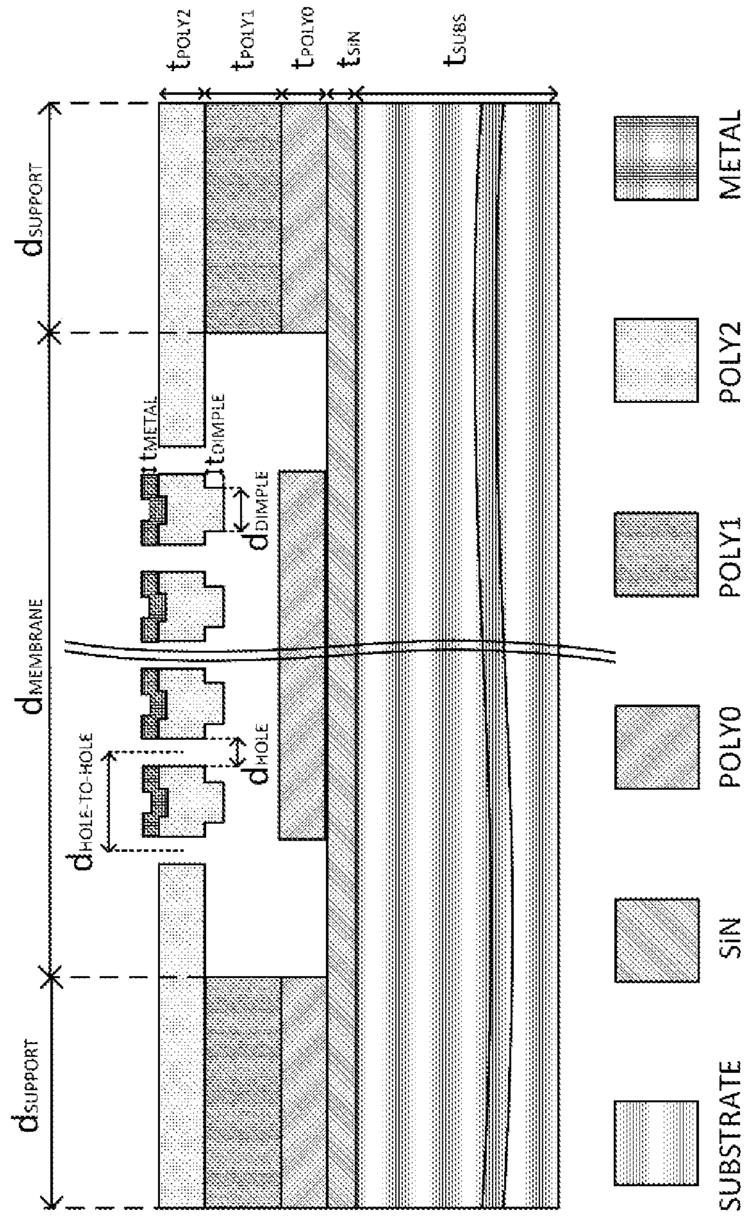

Figure 2

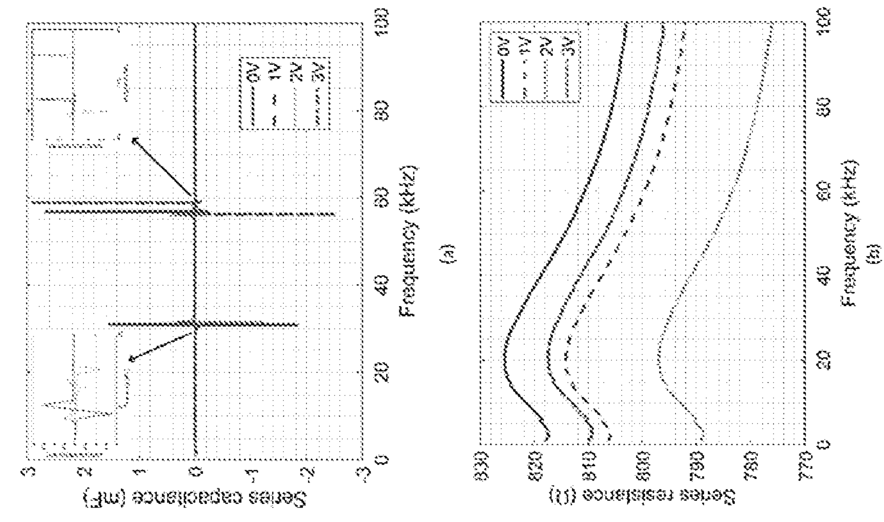

Figure 3b

Figure 3

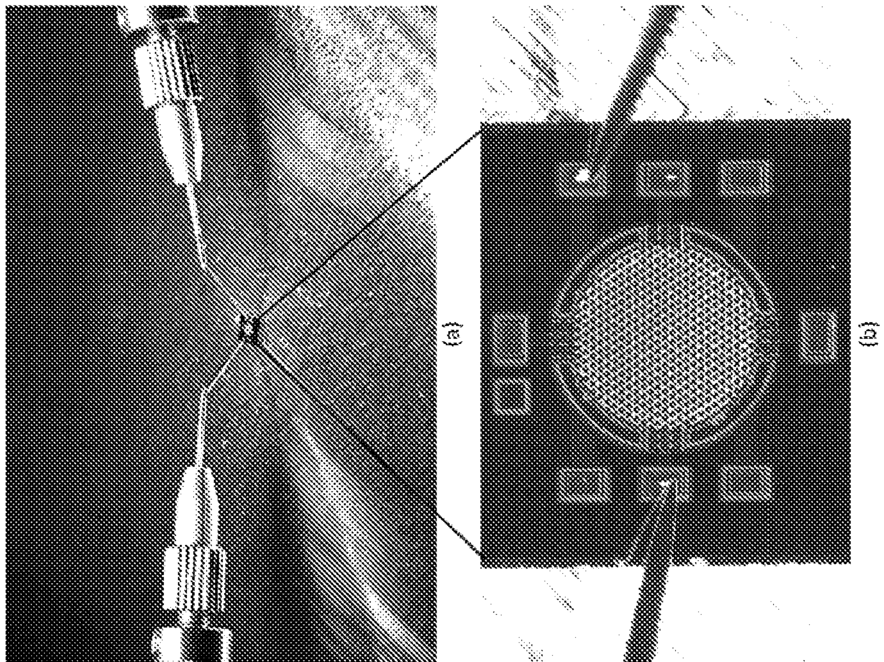

Figure 3a

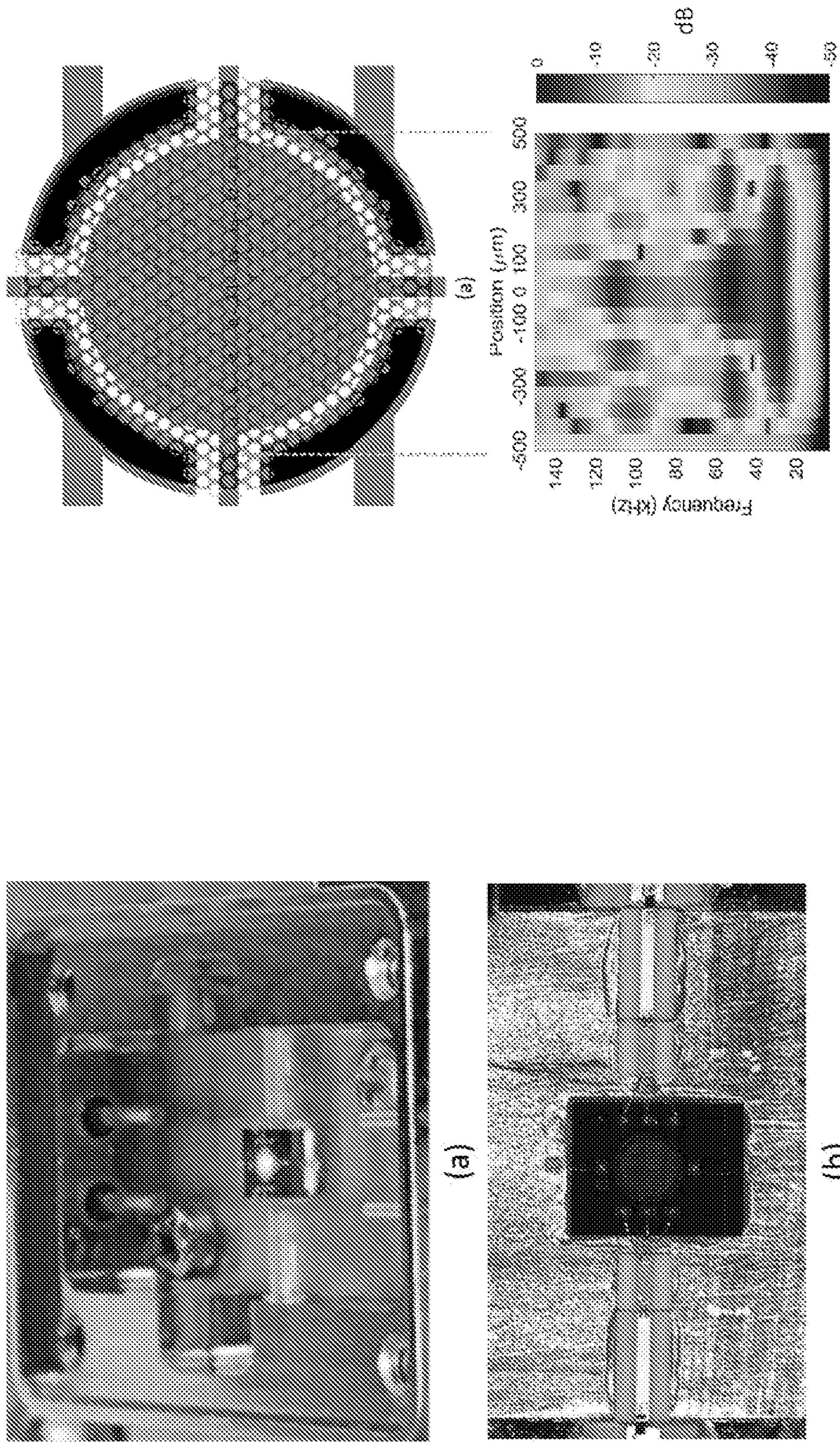

Figure 4

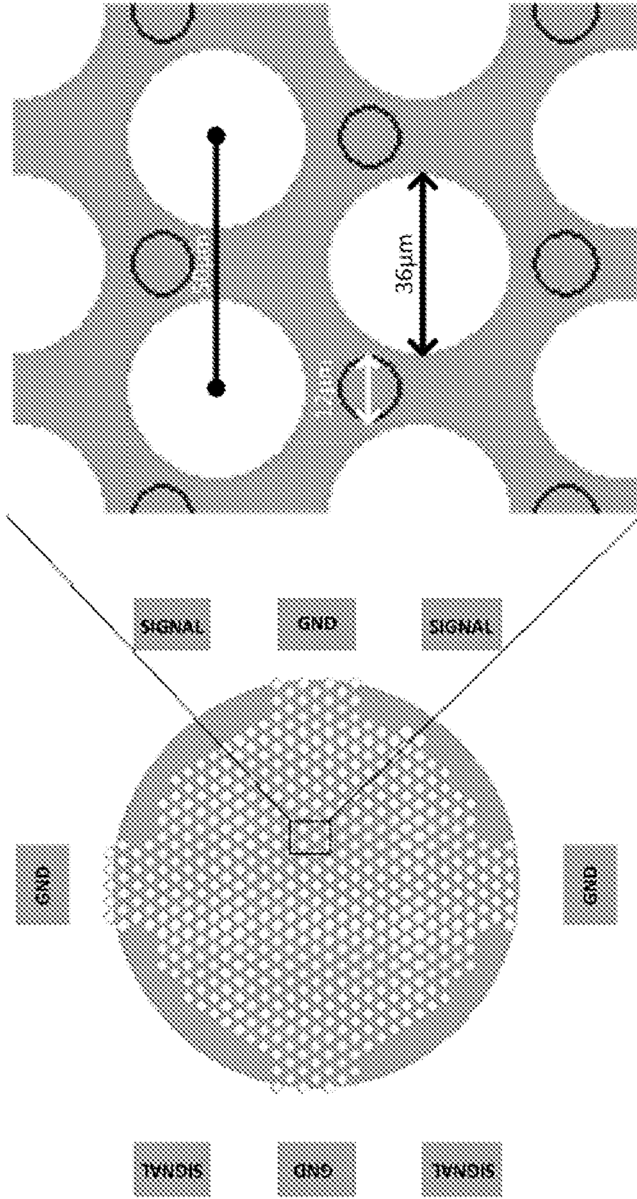

Figure 5a

Figure 5b

Figure 5.

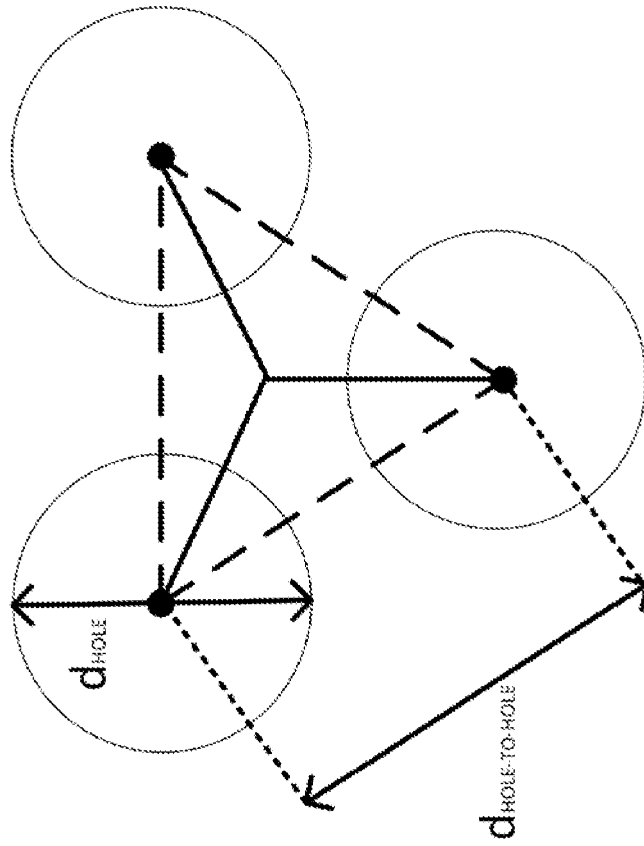

Figure 6

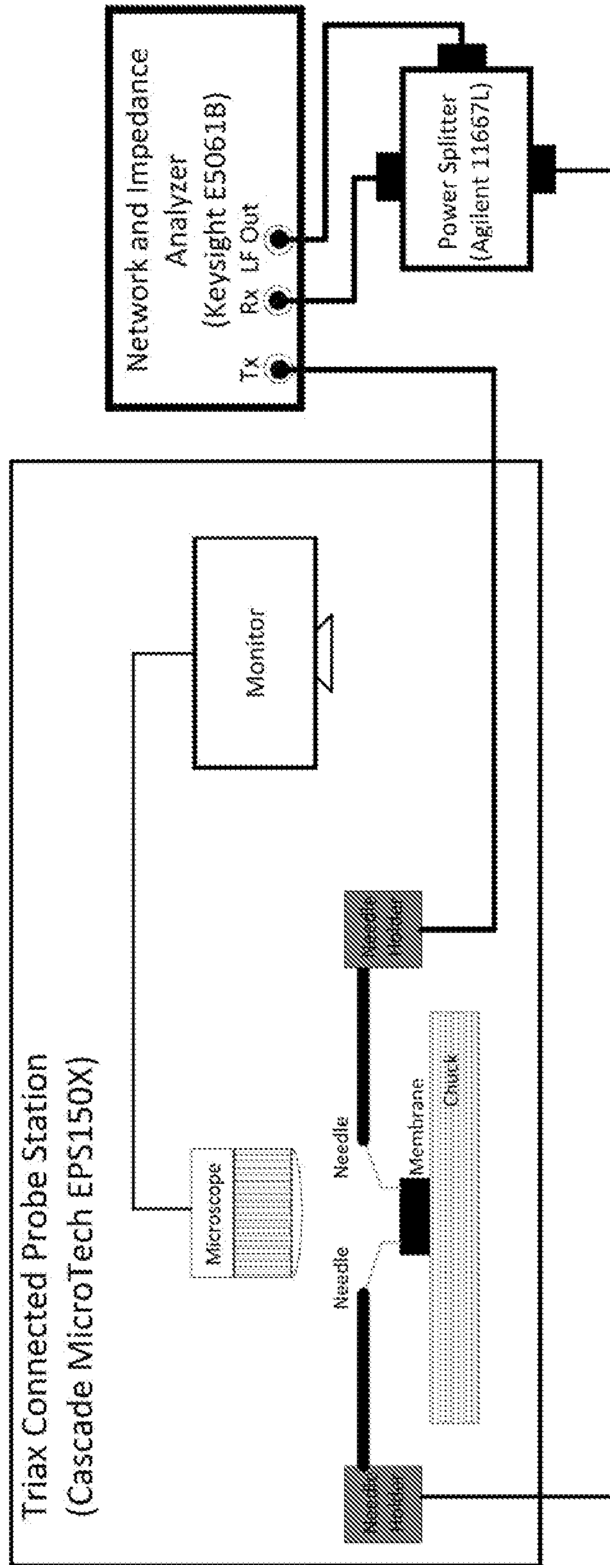

Figure 7

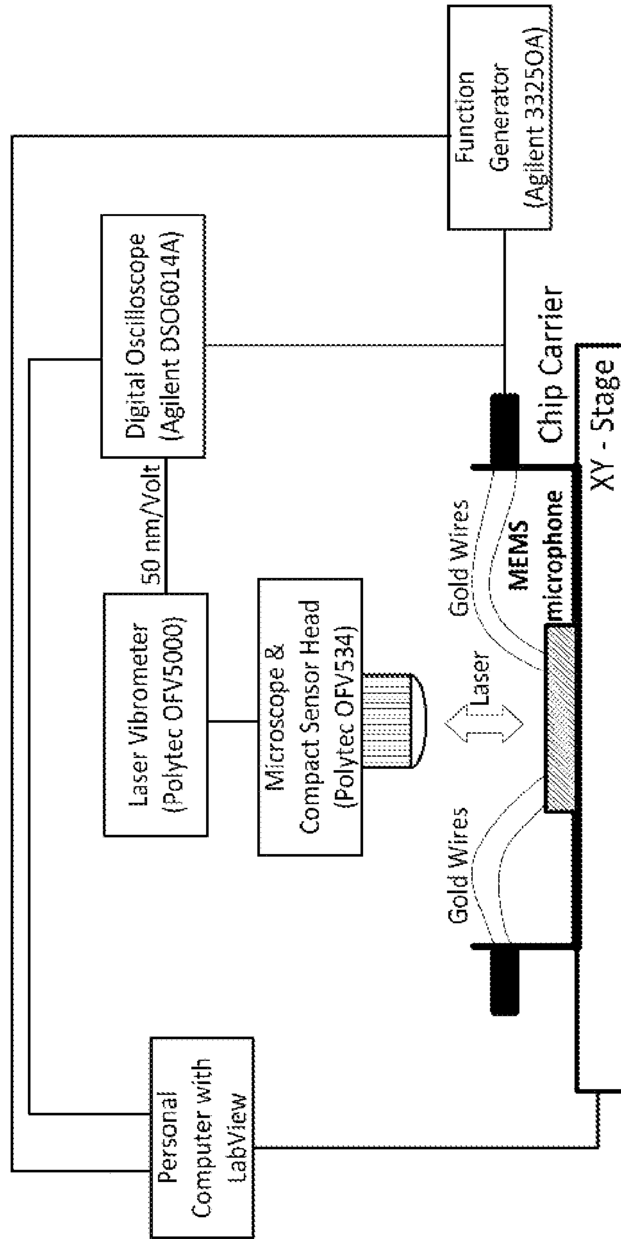

Figure 8

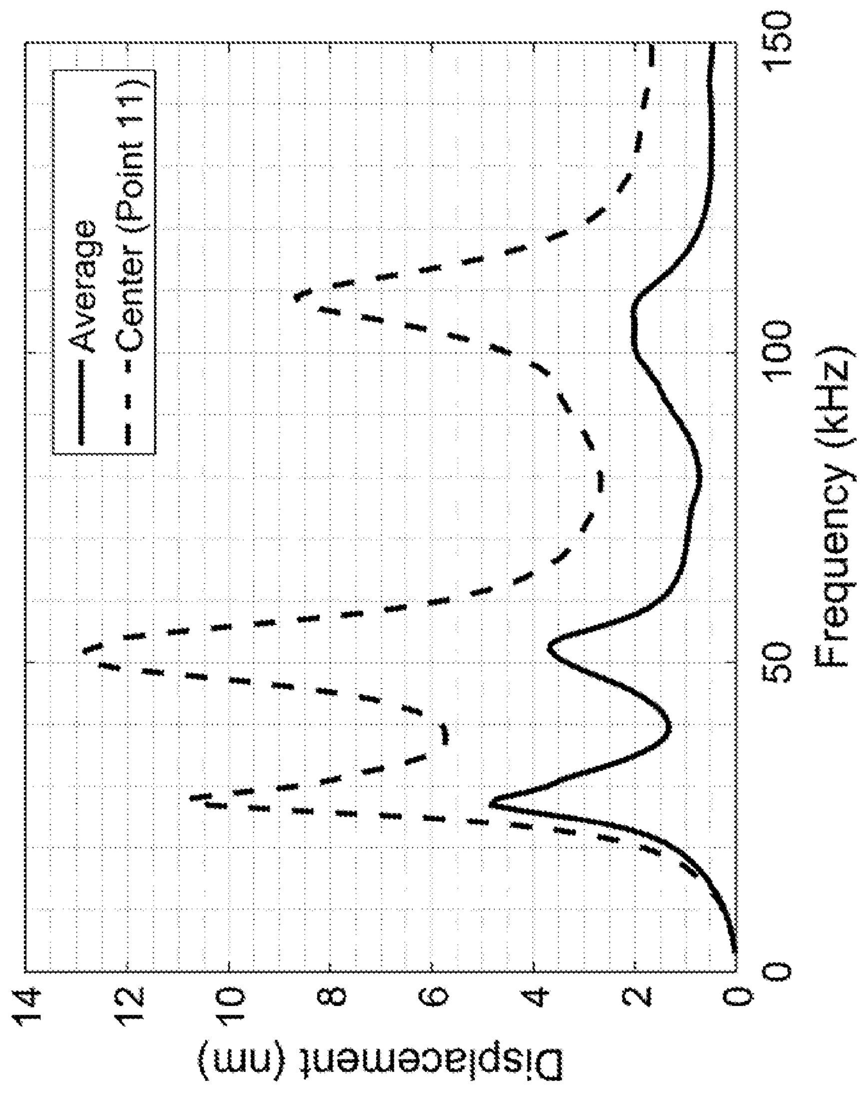

Figure 9

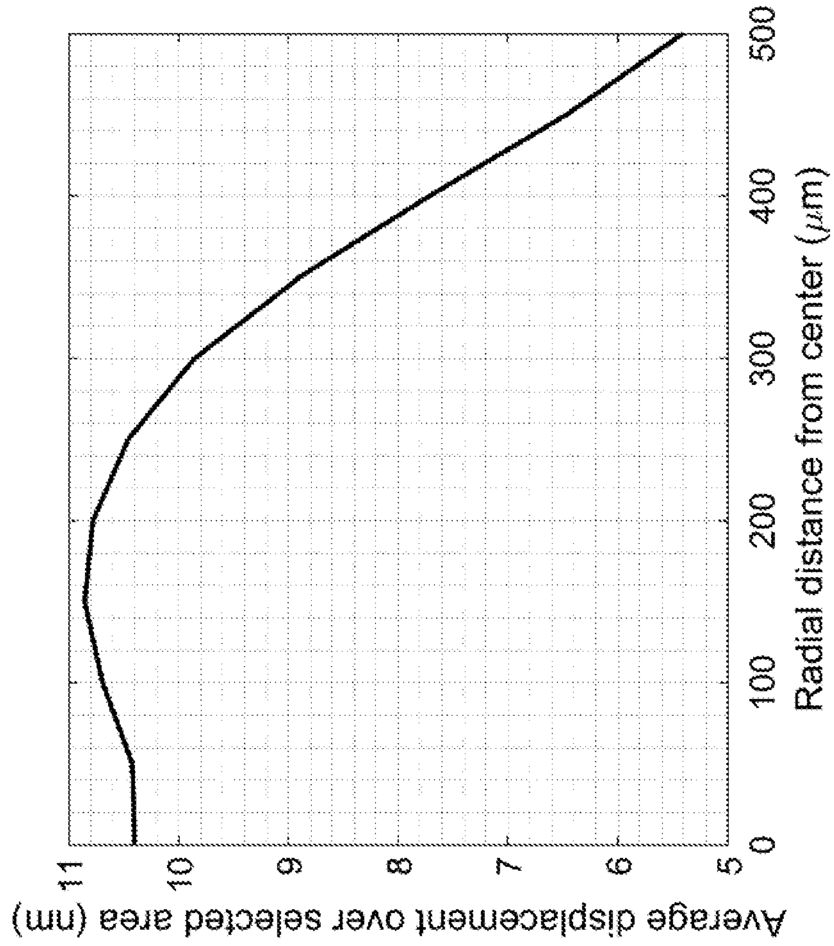

Figure 10

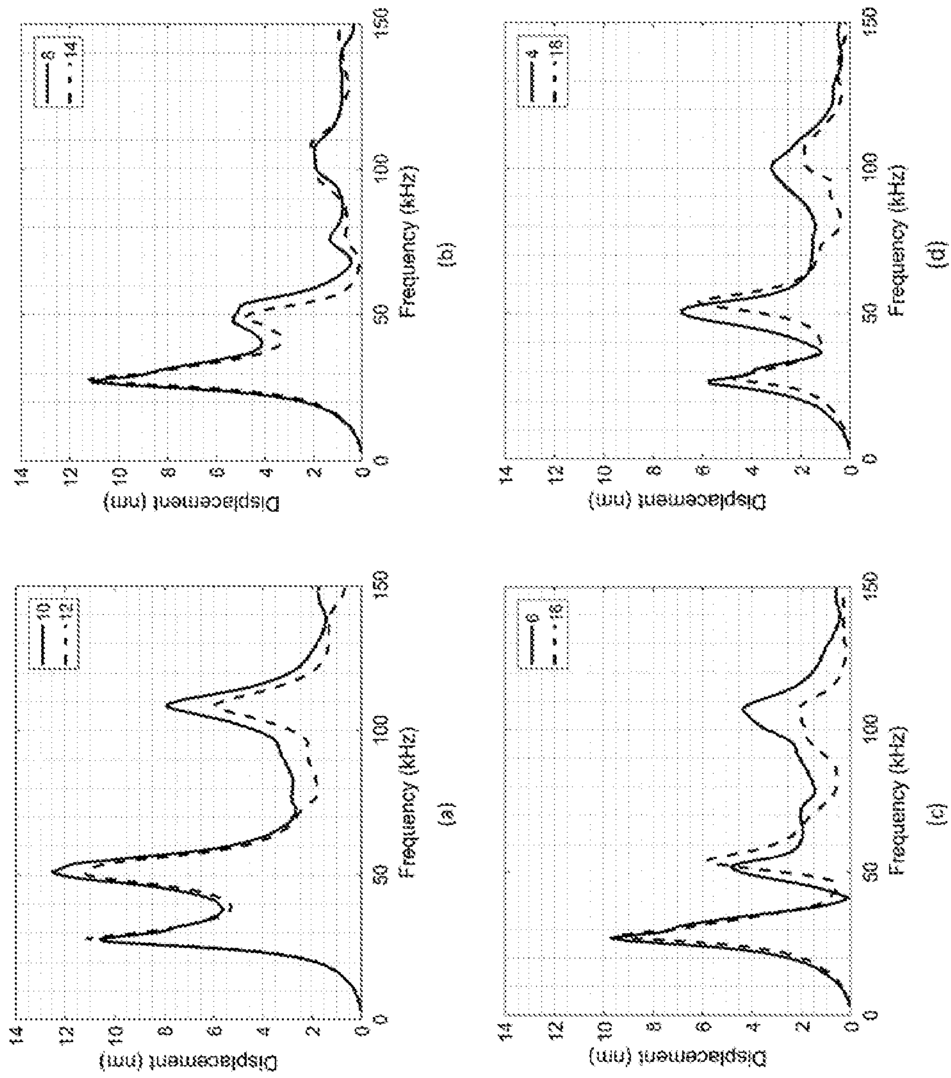

Figure 11

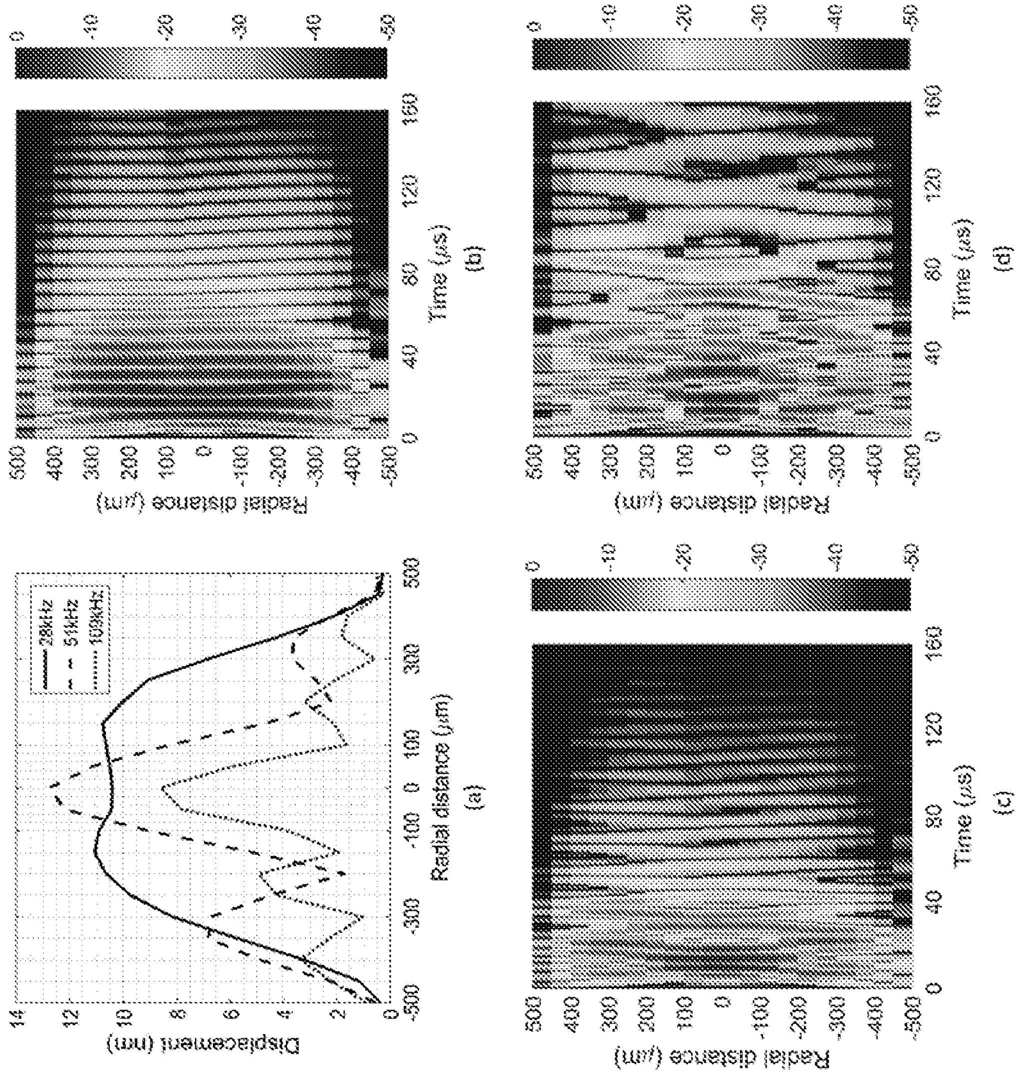

Figure 12

REFERENCES CITED IN THE DESCRIPTION

This list of references cited by the applicant is for the reader's convenience only. It does not form part of the European patent document. Even though great care has been taken in compiling the references, errors or omissions cannot be excluded and the EPO disclaims all liability in this regard.

Patent documents cited in the description

- US 6483619 B1 **[0008]**

Non-patent literature cited in the description

- **CHONGHUA ZHOU ; STEPHEN V. LETCHER ; ARUN SHUKLA.** Fiber-optic microphone based on a combination of Fabry-Perot interferometry and intensity modulation. *The J. Acoust. Soc. Am.,* 1995, vol. 98, 1042 **[0067]**
- **MING LI ; MING WANG.** Optical MEMS pressure sensor based on Fabry-Perot interferometry. *Optics Express,* 2006, vol. 14 (4 **[0067]**
- **JI-HUAN CHEN ; XU-GUANG HUANG ; JIA-RONG ZHAO ; JIN TAO ; WEI-XIN HE ; SONG-HAO LIU.** Fabry-Perot interference-based fiber-optic sensor for small displacement measurement. *Optics Communications,* 2010, vol. 283, 3315-3319 **[0067]**
- **J. A. BUCARO ; H. D. DARDY ; E. F. CAROME.** Fiber-optic hydrophone. *J. Acoust. Soc. Am.,* 1998, vol. 62, 1302 **[0067]**
- **QINGXU YU ; XINLEI ZHOU.** Pressure Sensor Based on the Fiber-Optic Extrinsic Fabry-Perot Interferometer. *Photonic Sensors,* 2011, vol. 1 (1), 72-83 **[0067]**
- **G.C FANGA ; P.G JIA ; Q. CAOA ; J.J XIONG.** MEMS Fiber-optic Fabry-Perot pressure sensor for high temperature application. *Proc. of SPIE,* 2016, vol. 10155, 101552H **[0067]**
- **ZHENFENG GONG ; KE CHEN ; XINLEI ZHOU ; YANG YANG ; ZHIHAO ZHAO ; HELIN ZOU ; QINGXU YU.** High Sensitivity Fabry-Perot Interferometric Acoustic Sensor for Low-Frequency Acoutic Pressure Detections. *J. Lightwave Tech.,* 2017, vol. 35 (24 **[0067]**
- **YU WU ; CAIBIN YU ; FAN WU ; CHEN LI ; JINHAO ZHOU ; YUAN GONG ; YUNJIANG RAO ; YUANFU CHEN.** A Highly Sensitive Fiber-Optic Microphone Based on Graphene Oxide Membrane. *J. Lightwave Tech.,* 2017, vol. 35 (19 **[0067]**
- **BIN LIU ; HAN ZHOU ; LEI LIU ; XING WANG ; MINGGUANG SHAN ; PENG JIN ; ZHI ZHONG.** An Optical Fiber Fabry-Perot Microphone Based on Corrugated Silver Diaphragm. *IEEE Transactions on Instrumentation and Measurement,* 2018, vol. 67 (8 **[0067]**
- **XUEQI LU ; YU WU ; YUAN GONG ; YUNJIANG RAO.** A miniature fiber-optic microphone based on annular corrugated MEMS diaphragm. *J. Lightwave Tech.,* 2018 **[0067]**
- **STEVE T. CHO ; KHALIL NAJAFI ; KENSALL D. WISE.** Internal Stress Compensation and Scaling in Ultrasensitive Silicon Pressure Sensor. *IEEE Transaction on Electron Devices,* 1992, vol. 39 (4 **[0067]**
- **M. GIOVANNI.** Flat and Corrugated Diaphragm Design Hand-book. 1982 **[0067]**
- **G. G. YARALIOGLU ; A. S. ERGUN ; B. BAYRAM ; E. HAEGGSTROM ; B. T. KHURI-YAKUB.** Calculation and measurement of electromechanical coupling coefficient of capacitive micromachined ultrasonic transducers. *IEEE Transactions on Ultrasonics, Ferroelectrics, and Frequency Control,* 2003, vol. 50 (4), 449-456 **[0067]**
- **I. O. WYGANT ; M. KUPNIK ; B. T. KHURI-YAKUB.** Analytically calculating membrane displacement and the equivalent circuit model of a circular CMUT cell. *IEEE Ultrasonics Symposium,* 2008, 2111-2114 **[0067]**